Title: Solvent-free microwave-assisted synthesis of tenorite nanoparticle-decorated multi-walled carbon nanotubes

Authors: Jennifer A. Rudd, Cathren E. Gowenlock, Virginia Gomez, Ewa Kazimierska, Abdullah M. Al-Enizi, Enrico Andreoli, Andrew R. Barron

PII: S1005-0302(19)30011-8
DOI: https://doi.org/10.1016/j.jmst.2019.01.002
Reference: JMST 1453

To appear in:

Received date: 17 July 2018
Revised date: 15 September 2018
Accepted date: 23 September 2018

Please cite this article as: Rudd JA, Gowenlock CE, Gomez V, Kazimierska E, Al-Enizi AM, Andreoli E, Barron AR, Solvent-free microwave-assisted synthesis of tenorite nanoparticle-decorated multi-walled carbon nanotubes, *Journal of Materials Science and amp; Technology* (2019), https://doi.org/10.1016/j.jmst.2019.01.002

Solvent-free microwave-assisted synthesis of tenorite nanoparticle-decorated multi-walled carbon nanotubes

Jennifer A. Rudd[a], Cathren E. Gowenlock[a], Virginia Gomez[a], Ewa Kazimierska[a], Abdullah M. Al-Enizi[b], Enrico Andreoli*[a], Andrew R. Barron[acd]

[a] Energy Safety Research Institute, Swansea University, Bay Campus, Swansea, SA1 8EN, UK

[b] Chemistry Department, College of Sciences, King Saud University, Riyadh, Saudi Arabia

[c] Department of Chemistry, Rice University, Houston, Texas 77005, USA

[d] Department of Materials Science and Nanoengineering, Rice University, Houston, Texas 77005, USA

* Author to whom correspondence should be addressed. E-mail address: E.Andreoli@Swansea.ac.uk (Enrico Andreoli).

[Received 71 July 2018; revised 15 September 2018; accepted 23 September 2018]

ABSTRACT

Copper-decorated carbon nanotubes (CNTs) have important applications as precursors for ultra-conductive copper wires. Tenorite-decorated CNTs (CuO-CNTs) are ideal candidate and are currently used in laborious processes. For this reason, we have developed a facile and scalable method for the synthesis of CuO-CNTs from copper acetate. It was found that the optimal loading of copper acetate onto the CNTs was 23.1 wt% and that three 1-minute microwave treatments were sufficient for the decomposition of copper acetate to copper

oxide. The loading of copper oxide onto the nanotubes was confirmed using X-ray photoelectron spectroscopy, energy-dispersive X-ray spectroscopy and thermogravimetric analysis. The materials were characterised using X-ray diffraction and scanning electron microscopy.

Keywords: microwave-assisted synthesis; multi-walled carbon nanotubes; tenorite; nanoparticle

1. Introduction

Ultra-conductive copper wire is gaining interest around the world for its increased electrical and thermal conductivity over traditional copper wire.[1-5] Ultra-conductive copper wire comprises copper and a nanocarbon material such as carbon nanotubes (CNTs) or graphene.[1, 6] In order to synthesise the quantities of ultra-conductive copper wire that will be required in the future it is vital that a facile and scalable manufacturing procedure is developed.

To date, copper and CNTs have been combined through surfactant templating,[7]where a surfactant is added to a mixture to control particle size; seeding,[8] where a particle deposits on the surface encouraging more of the sample particle to deposit in the same place; and solution stirring.[9] The use of these techniques, particularly surfactant templating and seeding, requires additives in the procedure, which increases the cost due to the additional chemicals and the time of the reaction in purifying the final product. In addition, the seeding technique requires the prior functionalization of the CNTs which adds significant time and cost, thereby decreasing the reaction scalability. Copper oxide decorated CNTs have previously been synthesised using three methods. The most common method, defined as molecular level mixing, is by stirring either copper acetate or copper nitrate with CNTs for several hours and then calcining at high temperature.[10-15] The less common methods are either mixing the two components and then using an autoclave at high temperature to convert copper acetate

(CuAc) to copper oxide (CuO)[16] or mixing the two components and then converting CuAc to CuO using sodium hydroxide.[17] A more efficient method of synthesizing copper oxide decorated CNTs is required. This article describes a facile and scalable method for the synthesis of CuO-CNTs, a precursor of ultra-conductive copper wire simply made from copper acetate and CNTs.

An efficient and scalable way to carry out reactions is by using microwaves. Microwaves have been used in chemical synthesis,[18-23] the processing of new materials[24-25] and in the purification of CNTs.[26] Carbon materials display a unique property under microwave irradiation in that they sustain a rapid temperature increase known as superheating.[27-30] CNTs, graphene and amorphous carbon nanoparticles have been reported to reach 1283 °C within one minute of irradiation,[31] leading to the generation of a highly localised nano-sized hot spot.[32] Achieving highly localised heating (*i.e.* delivering energy directly and precisely to a region of reduced dimensions) has long been a challenging objective in scientific research. This localised heat created on the surface of carbon nanomaterials can be used to decompose different metallic precursors resulting in the instantaneous formation of metal and metal oxide particles.[33-34] In this context, the addition of ferroferric oxide, ferrite composites or nickel oxide to multi-walled CNTs (MWCNTs) has been shown to increase the microwave absorption capacity of CNTs.[35-36] Whilst copper and copper oxide particles have previously been prepared in solution synthesis under microwave irradiation,[37-38] this procedure required the use of solvent and 30 minutes of irradiation.

In this work, we describe a facile and scalable one-pot synthesis of copper oxide decorated CNTs using microwave treatment. The superheating and selective heating properties of carbon nanomaterials were used to create hybrid materials in a solvent-free synthesis process. The application of nanomaterials as both heating sources and reagent substrates are novel uses of microwave radiation. Using this technique metallic oxide nanoparticles have

been created on the surface of the multi-walled CNTs. The amount of copper in the final products was easily tuned by changing the initial amount of copper precursor.

2. Experimental

2.1. Materials and methods

Copper(II) acetate monohydrate $Cu(CO_2CH_3)\cdot H_2O$ was purchased from Sigma-Aldrich and used as received. MWCNTs were prepared using a table top horizontal tube reactor (Nanotech Innovations SSP-354) as previously reported[26, 39] and cleaned following the procedure described in ref. 22. Water was purified before use with an Elix Milliport AFS 15E Water Purification System (ρ > 15 MΩ/cm).

Sample morphology and elemental composition were examined using field emission gun scanning electron microscopy (FEG-SEM JEOL 7800F) and quantitative energy-dispersive X-ray (EDX) spectroscopy under a Hitachi Field Emission S-4800 SEM, both equipped with an Oxford Instruments Inca EDX detector. For analysis *ca.* 3 mg of sample was pressed into indium foil. The indium foil was then fixed to a carbon tab. Transmission electron microscopy was performed under a JEOL JEM-1011.

X-ray photoelectron spectra (XPS) were recorded under a Kratos Axis Supra instrument using a monochromatic Al-K_α source (1486.69 eV). All spectra were recorded using a charge neutraliser to limit differential charging and subsequently calibrated to the main indium peak at a binding energy of 443.8 eV. Survey scans were recorded at a pass energy of 160 eV and high-resolution data at a pass energy of 20 eV. Data were fitted using CASA XPS software with Shirley backgrounds. X-ray diffraction (XRD) patterns were recorded on a Brüker D8 DISCOVER diffractometer in Bragg–Brentano geometry with a Cu-K_α X-ray source (λ = 0.15418 nm) and analysed using Match 2 software.

Thermogravimetric analyses (TGA) were carried out using a TA Instruments SDT Q600 thermogravimetric analyser. All samples were purged under a 100 mL/min flow of argon for 1 h and 25 °C then ramped at 10 °C/min to 100 °C, where they remained for 1 h under 100

mL/min flow of argon to dry. The gas was then switched to air at a flow rate of 100 mL/min while the temperature was held at 100 °C for another 5 min. Then, the temperature was ramped at a rate of 10 °C/min to 900 °C.

2.2. Preparation of tenorite-decorated MWCNTs

10 mg of MWCNTs were placed into a glass vial. A stock solution of copper acetate in water (concentration 1 mg/mL) was prepared and the appropriate volume of solution (e.g., 9 mL = 9 mg CuAc solution to give a copper acetate loading of 47.4 wt%) added to create a range of loadings of CuAc on MWCNTs (Table 1). The vial containing the CuAc and MWCNTs was then sonicated for 15 min. Afterwards, the vial was transferred to an oven for 4 h at 80 °C to evaporate the water and dry the sample. After cooling to room temperature, the vial was placed in a microwave (Panasonic NN-CT579SBPQ) and given the required number of 1-minute microwave treatments at 1000 Watts. Two Pyrex beakers containing water were placed in the microwave during the microwave treatments, one each side of the vial, to prevent overheating.

3. Results and discussion

A schematic diagram of the preparation of tenorite-decorated MWCNTs is shown in Fig. 1. The copper acetate was added as an aqueous solution to a vial containing 10 mg MWCNT. The CuAc was solubilised to achieve good dispersion over the nanotubes. Ultra-sonication was then used to disperse the nanotubes in the solvent and enable homogeneous deposition of the CuAc onto the nanotubes. The water was removed by oven-drying the sample at 80 °C for 4 h. During this time it was expected that the CuAc particles would settle onto the CNTs as the solvent slowly evaporated. Finally, the sample was treated with 3 x 1-minute microwave treatments to decompose the CuAc to tenorite through the superheating effect of the microwave-nanotube combination.

3.1. Method development

The presence of copper oxide particles on MWCNTs was confirmed using FEG-SEM and EDX. Fig. 2 shows nanoparticulate deposits of copper oxide on and in-between MWCNTs after microwaving in the presence of 47.4 wt% copper acetate. High magnification micrographs show particles that are quasi-spherical in shape and polycrystalline in nature, as shown in Fig. 3. This observation agrees well with literature reports on copper oxide particles from microwave assisted synthesis.[40] The average size of such agglomerates was between 200-300 nm and closer analysis revealed that the agglomerates consisted of particles approximately 20 nm in diameter. Some layered copper oxide nanoparticles were also identified in the samples (Fig. S1).

To confirm that the nanoparticles were made of copper and oxygen, elemental analysis was carried out using EDX. A sample was scanned and mapped to allow for the selection of areas with high copper and oxygen content, as shown in Fig. 3(a-b). Fig. 3(c) shows the elemental map resulting from the superposition of all elements (C, Cu, O, Fe, and In) detected in the selected area. The presence of iron was due to the catalyst used in the synthesis of MWCNTs, while indium was used to hold the sample in place during the analysis. Fig. 3(d-f) shows that copper and oxygen (but no carbon) were detected in the nanoparticle, supporting the formation of tenorite. This was further supported by calculating the molar ratio of copper and oxygen from the EDX spectrum shown in Fig. 3(d). Copper (39.5 wt%) and oxygen (13.1 wt%) were detected in 1:1.3 molar ratio, close to the 1:1 ratio of tenorite. Clusters of amorphous carbon were also found, resulting from the thermal decomposition of acetate during microwaving, as evident in Fig. 3(a).

In addition to the agglomerates of copper oxide nanoparticles observed by SEM, single nanoparticles of ~10 nm diameter can be observed by transmission electron microscopy (TEM) in samples of all wt% Cu. The nanoparticles are encased in carbon caused by the decomposition of the acetate group of the starting material copper acetate (Fig. 4). The

distribution of copper encased in carbon appears homogeneous over a large area of the nanotubes (Fig. S2).

To ascertain the required number of microwave treatments, we investigated two different loadings of CuAc onto the MWCNTs, specifically 9 mg (47.4 wt%) and 1 mg (9.1 wt%). We then analysed the conversion of copper acetate to copper oxide using thermogravimetric analysis (Fig. S3), the results are collected in Fig. 5. For the lower loading (9.1 wt%) after one microwave treatment a significant proportion of the copper acetate was converted to copper oxide, with only 3.1% of the sample weight remaining as copper acetate. After three treatments all CuAc was converted to copper oxide. However, at the higher loading of 47.4 wt% one microwave treatment resulted in 22.2% of the sample weight remaining as copper acetate. After five microwave treatments nearly all the copper acetate was converted to copper oxide, with only 3.3% of the total sample weight remaining as copper acetate. As this was the highest loading that we intended to use it was determined that three 1-min microwave treatments would be sufficient to convert the copper acetate to copper oxide in samples of lower loadings. This decision would also make the process more efficient as unnecessary microwave treatments were avoided.

XRD was used to confirm that copper acetate was converted to tenorite upon microwaving in the presence of MWCNTs. The XRD diffraction patterns of a 47.4 wt% sample and of as received MWCNTs after three microwave treatments are shown in Fig. 6. The CNTs showed diffraction peaks at 26° and 43° corresponding to the (002) and (100) reflections of the graphite layers structure.[41-42] Decorated CNTs with copper oxide nanoparticles show peaks at 35.4° and 38.7° that correspond to the (002) and (111) reflections related with tenorite.[43] The large peak at 30° is due to amorphous species. This peak is not observed in the pattern of the MWCNTs, leading us to attribute the broad peak to amorphous carbon formed from the decomposition of the acetate portion of CuAc, visible in Fig. 3(a). Lin *et al.* reported the decomposition of the acetate to carbon dioxide at temperatures of 400 °C.[44] However, when

the copper acetate is in close contact with the MWCNTs under microwave irradiation the localised temperature can reach 1283 °C.[31] At these elevated temperatures the acetate appears to turn directly to amorphous carbon. There is additional evidence for this in the TGA analyses (*vide infra*).

3.2 Materials design

After confirming the decoration of CNTs with tenorite and determining the number of microwave treatments required, we investigated the effects of adding different amounts of copper acetate. Varying quantities of copper acetate (0-47.4 wt%) were added to a fixed amount (10 mg) of CNTs (Table 1). The atomic weight percent of copper decorating the CNTs for 9.1, 16.7, 23.1 and 37.5 wt% was quantified before and after microwave treatment using EDX, as shown in Fig. 6. The atomic weight percent of copper is reported with respect to the total amount of copper plus carbon detected in the sample. Within the spread of data, the amount of copper on the CNTs is the same before (red circles and bars) and after microwave treatment (black circles and bars). Independent of microwave treatment, the surface of the sample becomes less homogenous with increasing amounts of copper added to the MWCNTs. This is evidenced by the increased spread of the data at higher loadings, *i.e.* the range bars are wider at higher CuAc loading. Notably, the EDX detected significantly less copper in the MWCNT samples than the amount loaded during preparation. For example, only 1.5 at. wt% copper was detected for the sample loaded with 14.9 at. wt% copper during preparation. The same disparity was observed using XPS. However, a good agreement between 'as-prepared copper loading' and 'measured copper loading' was found using TGA (*vide infra*). Therefore, a large amount of the copper was confined in the bulk of the sample.

To probe the characteristics of the surface of the tenorite-decorated CNTs, XPS was carried out for each sample after microwave treatment. XPS confirmed the presence of copper and carbon. The copper regions from the XPS data were fitted using a standard Gaussian-Lorentzian (GL-30) fit (Fig. 8). The presence of shake-up satellites is characteristic of copper(II) and this confirms that the copper in the sample is copper(II) oxide (tenorite). The signals

corresponding to Cu($2p_{1/2}$) and Cu($2p_{3/2}$) are centred at 953 eV and 934 eV, respectively. Fitting the carbon (1s) peak in the XPS data output was non-trivial. The presence of CNTs in the sample resulted in an asymmetric carbon peak. This meant that a mixed Doniach-Sunjik Sum Gaussian Lorentzian fitting had to be applied, following the precedent detailed in the paper by Kalbac et al.[45] The C(1s) peak was predominantly sp^2 and contained an additional peak between 286 and 293 eV, attributed to a mix of plasmon loss and $\pi \rightarrow \pi^*$ transitions. The peak at 284 eV is due to the amorphous carbon caused by decomposition of the acetate group of CuAc.

As depicted in Fig. 9, the amount of copper decorating the MWCNTs increases between 0.3 and 8.4 at. wt% of added copper from CuAc. In addition, samples show good homogeneity in the same loading range. Beyond 8.4 at. wt% the samples become inhomogeneous, consisting of a mixture of dense and sparse patches of tenorite decoration, giving rise to the large spread. Six data points were gathered for each of the 14.6 and 19.4 at. wt% samples to confirm such a disparity was real. For the XPS measurements three wide scans were taken per sample and compared. The wide scans overlapped in intensity for both copper and carbon signals and so only one region scan per sample was measured. The amount of copper decorating the MWCNTs follows the same trend in the XPS and EDX results, and the majority of the XPS results fall within the spread observed in the EDX results. These findings indicate that when copper nanoparticle-decorated MWCNTs are embedded into indium foil for EDX and XPS analyses, a single XPS measurement is representative. However, as the sampling width of XPS is *ca.* 1 mm the inhomogeneity of the surface is averaged out. In contrast, EDX measures a smaller sample area (*ca.* 1 μm^2) but to a greater depth (*ca.* 500 µm for EDX versus 0.01 µm for XPS). Therefore, with EDX, multiple measurements are required to obtain the average amount of copper decoration of the MWCNTs but an estimate of the spread of decoration can be achieved.

To assess the loading of copper in the bulk of the composites, MWCNTs with a range of loadings of CuAc (0 wt%, 9.1 wt%, 23.1 wt% and 47.4 wt%) microwaved three times, and a control sample of pure CuAc, were analysed using TGA (Fig. 10). The thermogram of pure CuAc shows two weight loss steps below 350 °C. The first step, between 100 and 170°C, is caused by dehydration of the copper acetate monohydrate (labeled "H_2O loss").[44] The weight loss is non-stoichimetric (*i.e.*, molar ratio CuAc:H_2O = 1:1) as the microwave treatments heated the samples sufficiently to remove some water of crystallization (additionally, the samples were pre-treated at 100 °C to remove water from the surface of MWCNTs). The second step, with a weight loss of *ca.* 60.6% between 200 and 300°C, corresponds to the decomposition of the anhydrous copper acetate to a mixture of cupric oxide, cuprous oxide and copper metal (labeled "Ac decomposition").[44] This is in good agreement with the stoichiometric weight loss of 59.1%. Finally a weight increase of 10.5% was observed between 300 and 500°C, corresponding to the oxidation of Cu and Cu_2O to CuO (labeled "CuO formation").[44]

The thermogram of the MWCNTs + 9.1 wt% CuAc is like that of as received MWCNTs (no CuAc) and does not show a weight loss between 200 and 300 °C, indicating that the three microwave treatments have converted all the copper acetate to copper oxide at this loading of CuAc (Fig. 9). The 23.1 wt% and 47.4 wt% MWCNT samples however, do show weight losses from 200 to 300 °C with 5.5 and 7.5% CuAc still remaining in the samples after three microwave treatments. All MWCNT samples show a weight loss from 400 to 650 °C consistent with oxidation of the nanotubes (labeled "CNT decomposition").[26] This weight loss occurs at slightly different temperatures dependent on the original loading of copper acetate on the CNTs. This is due to an increase in the amount of amorphous carbon present[26] from the decomposition of the acetate moiety in the microwave, as observed in the SEM and XRD characterisations (Figs. 3 and 6). The higher the original loading of copper acetate onto the MWCNTs the more amorphous carbon present and, therefore, the lower the temperature of the weight loss. The residue remaining after TGA comprises iron oxide

and copper oxide. All MWCNT samples contain a residue of iron catalyst particles from the MWCNT synthesis method. The quantity of iron residue was determined by TGA to be 2.3 wt% (Fig. S4).

The amount of copper present in the MWCNT samples was calculated from TGA analyses (see Section 5 in the SM for details) and plotted against the as-prepared loading of copper from CuAc added to the nanotubes, as shown in Fig. 11. The TGA of the bulk samples confirms a good loading of copper onto the MWCNTs after three microwave treatments. The amount of copper oxide decorating the MWCNTs increased rapidly with increasing copper acetate loading up 23.1 wt% (corresponding to an as-prepared copper loading of 8.4 at. wt%, see Table 1) and then leveled off at higher loadings. The deviation from the expected copper loading, shown in Fig. 11 with a dashed diagonal line, results from a trade-off of two key processes: (i) the conversion CuAc to tenorite, and (ii) the combustion of carbon at high temperature during microwaving. Acetate combustion appears significant at lower loadings where all CuAc is converted to copper oxide, thus the positive deviation from the diagonal line. It follows that up to a CuAc loading of 23.1 wt%, most of the loaded copper decorates the MWCNTs. After this value, the nanotubes start being saturated and the further uptake of copper on the nanotubes becomes less efficient.

4. Conclusions

The objective of this study was to synthesise copper oxide-decorated CNTs in a facile one-pot microwave assisted synthesis. We have shown that it is possible to decompose copper acetate to copper oxide using microwaves and generate tenorite-decorated MWCNTs through a simple process which is easily scalable. SEM analysis proved the formation of nanometre sized (diameter in range of 200-300 nm) particles of CuO built of approximately 20 nm particles. EDX and XPS analyses confirmed that copper oxide was formed. When 0.9-23.1 wt% of copper acetate is added to MWCNTs the resulting copper oxide particles are well dispersed over the surface of MWCNTs giving a homogenous sample. However, addition of above 23.1 wt% copper acetate leads to an inhomogeneous surface with patches of dense

and sparse copper oxide coverage. The samples were analysed using EDX, XPS and TGA to determine the exact quantity of copper deposited onto MWCNTs, and the average maximum loading achieved was 17.2 at. wt% for the 19.4 wt% added CuAc sample. It was determined, by EDX measurements of the sample, before and after the microwave treatment, that the MWCNTs reach a saturation point above 17.2 wt% added CuAc above which no further copper uptake was observed. Further work will therefore seek to improve the uptake of copper by MWCNTs at higher loadings. We are now testing the same solvent-free microwave synthetic approach with high purity single-walled CNTs. The resulting tenorite-decorated tubes will be reduced to copper metal-decorated MWCNTs to be used in the preparation of ultra-conductive copper.

Acknowledgments

The authors gratefully acknowledge the financial support provided by the Welsh Government Sêr Cymru National Research Network in Advanced Engineering and Materials (NRN-150) and the Sêr Cymru Chair Programme (A.R.B.). The Welsh Government is also acknowledged for the Sêr Cymru II Fellowship (C.E.G.) and the Sêr Cymru II Recapturing Talent Fellowship (E.K.) both partly funded by the European Regional Development Fund (ERDF). This work is also part of the Flexible Integrated Energy Systems (FLEXIS) and Reduce Industrial Carbon Emissions (RICE) research operations funded by the Welsh European Funding Office (WEFO). Financial support was also provided by the Engineering and Physical Sciences Research Council (EPSRC) UK, the Robert A. Welch Foundation (C-0002), and King Saud University. We would like to acknowledge the assistance provided by the Swansea University AIM Facility, which was funded in part by the EPSRC (EP/M028267/1), the European Regional Development Fund through the Welsh Government (80708) and the Sêr Solar project via the Welsh Government. We thank Dr James Mcgettrick and Dr Daniel Jones for XPS support.

REFERENCES

1. D.F. Lee, M. Burwell, H. Stillman, Priority research areas to accelerate the development of practical ultra-conductive copper conductors. *Oak Ridge National Laboratory,* **2015**.
2. O. Hjortstam, P. Isberg, S. Söderholm, H. Dai, *Appl. Phys. A 78 (***2004)** 1175-1179.
3. N. Banno, T. Takeuchi, *Journal of the Japan Institute of Metals and Materials 73 (***2009)** 651-658.
4. K. Koziol, Ultrawire Final Report Summary, *European Commision Community Research and Development Information Service,* **2016**.
5. W.A.D.M. Jayathilaka, A. Chinnappan, S. Ramakrishna, *J. Mater. Chem. C 5 (***2017)** 9209-9237.
6. C. Subramaniam, T. Yamada, K. Kobashi, A. Sekiguchi, D.N. Futaba, M. Yumura, K. Hata, *Nat. Commun. 4 (***2013)** 2202.
7. J.J. Brege, C.E. Hamilton, C.A. Crouse, A.R. Barron, *Nano Lett. 9 (***2009)** 2239-2242.
8. K.D. Wright, C.E. Gowenlock, J.C. Bear, A.R. Barron, *ACS Appl. Mater. Interf. 9 (***2017)** 27202-27212.
9. O. Baturina, Q. Lu, F. Xu, A. Purdy, B. Dyatkin, X. Sang, R. Unocic, T. Brintlinger, Y. Gogotsi, *Catalysis Today 288* (Supplement C) *(***2017)** 2-10.
10. Z. Yu, J. Meng, Y. Li, Y. Li, *Int. J. Hydrogen Energ. 38 (***2013)** 16649-16655.
11. D.W.Kim, K.Y. Rhee, S.J.Park, *J. Alloy. Compd. 530* (Supplement C) *(***2012)** 6-10.
12. M. Gopiraman, S. Ganesh Babu, Z. Khatri, W. Kai, Y.A. Kim, M. Endo, R. Karvembu, I.S. Kim, *Carbon 62* (Supplement C) *(***2013)** 135-148.
13. H.Q. Wu, X.W. Wei, M.W. Shao, J.S. Gu, M.Z. Qu, *Chem. Phys. Lett. 364 (***2002)** 152-156.
14. K.T.Kim, S.I. Cha, T. Gemming, J. Eckert, S.H. Hong, *Small 4 (***2008)** 1936-1940.
15. S.I. Cha, K.T. Kim, S.N. Arshad, C.B. Mo, S.H. Hong, *Adv. Mater. 17 (***2005)** 1377-1381.
16. M. Asad, M.H. Sheikhi, *Sensor. Actuator. B: Chem. 231* (Supplement C) *(***2016)** 474-483.
17. Y. Zhao, M. Ikram, J. Zhang, K. Kan, H. Wu, W. Song, L. Li, K. Shi, *Appl. Surf. Sci. 428* (Supplement C) *(***2018)** 415-421.
18. V. Gomez, A.M. Balu, J.C. Serrano-Ruiz, S. Irusta, D.D. Dionysiou, R. Luque, J. Santamaría, *Appl. Catal. A 441* (Supplement C) *(***2012)** 47-53.
19. C.C.Landry, A.R. Barron, *Science 260 (***1993)** 1653.
20. C.C.Landry, J. Lockwood, A.R. Barron, *Chem. Mater. 7 (***1995)** 699-706.
21. L. Zhang, J. Lan, J. Yang, S. Guo, J. Peng, L. Zhang, C. Zhou, S. Ju, *J. Mater. Sci. Technol. 33 (***2017)** 874-878.
22. X. Shen, Y. Zhai, Y. Sun, H. Gu, *J. Mater. Sci. Technol. 26 (***2010)** 711-714.
23. Q. Zhu, Y. Zhang, J. Wang, F. Zhou, P.K. Chu, *J. Mater.Sci. Technol. 27 (***2011)** 289-295.
24. V. Gomez, C.W. Dunnill, A.R. Barron, *Carbon 93* (Supplement C) *(***2015)** 774-781.
25. W.L. Song, M.S. Cao, Z.L. Hou, X.Y. Fang, X.L. Shi, J. Yuan, *Appl. Phys. Lett. 94 (***2009)** 233110.
26. V. Gomez, S. Irusta, O.B. Lawal, W. Adams, R.H. Hauge, C.W. Dunnill, A.R. Barron, *RSC Adv. 6 (***2016)** 11895-11902.
27. F.G. Brunetti, M.A. Herrero, J.d.M. Muñoz, A. Díaz-Ortiz, J. Alfonsi, M. Meneghetti, M. Prato, E. Vázquez, *J. Am. Chem. Soc. 130 (***2008)** 8094-8100.
28. A.L. Higginbotham, P.G. Moloney, M.C. Waid, J.G. Duque, C. Kittrell, H.K. Schmidt, J.J. Stephenson, S. Arepalli, L.L. Yowell, J.M. Tour, *Comp. Sci. Technol. 68 (***2008)** 3087-3092.
29. J. Guo, Y. Duan, L. Liu, L. Chen, S. Liu, *J. Electromag. Anal. Appl. 03 (***2011)** *No.05*, 7.
30. B. Wen, M.S. Cao, Z.L. Hou, W.L. Song, L. Zhang, M.M. Lu, H.B. Jin, X.Y. Fang, W.Z. Wang, J. Yuan, *Carbon 65 (***2013)** 124-139.
31. K. MacKenzie, O. Dunens, A.T. Harris, *Sep. Purif. Technol. 66 (***2009)** 209-222.
32. J. Gracia, M. Escuin, R. Mallada, N. Navascues, J. Santamaria, *Nano Energy 20* (Supplement C), *(***2016)** 20-28.
33. Y. Lin, D.W. Baggett, J.W. Kim, E.J. Siochi, J.W. Connell, *ACS Appl. Mater. Interf. 3 (***2011)** 1652-1664.
34. G. Qiu, S. Dharmarathna, Y. Zhang, N. Opembe, H. Huang, S.L. Suib, *J. Phys. Chem. C 116 (***2012)** 468-477.

35.M.S. Cao, J. Yang, W.L. Song, D.Q. Zhang, B. Wen, H.B. Jin, Z.L. Hou, J. Yuan, *ACS Appl. Mater. Interf. 4 (***2012)** 6949-6956.
36.P.J. Liu, Z.J. Yao, V. Ming Hong Ng, J.T. Zhou, Z.H. Yang, L.B. Kong, *Acta Metall. Sinica Engl. Lett. 31 (***2018)** 171-179.
37.A.M. Raspolli Galletti, C. Antonetti, M. Marracci, F. Piccinelli, B. Tellini, *Appl. Surf. Sci. 280* (Supplement C) *(***2013)** 610-618.
38.N. Leelaviwat, S. Monchayapisut, C. Poonjarernsilp, K. Faungnawakij, K.S. Kim, T. Charinpanitkul, *Curr. Appl. Phys. 12 (***2012)** 1575-1579.
39.A.W. Orbaek, N. Aggarwal, A.R. Barron, *J. Mater. Chem. A 1 (***2013)** 14122-14132.
40.P. Sutradhar, M. Saha, D. Maiti, *J. Nanostruct. Chem. 4 (***2014)** 86.
41.O. Hassel, *Zeitschrift fuer Physik 25 (***1924)** 317-337.
42.P. Trucano, R. Chen, *Nature 258 (***1975)** 136-137.
43. P. Niggli, *Kristallgeometrie, Kristallphysik, Kristallchemie 57 (***1922)** 253-299.
44. Z. Lin,; D. Han,; S. Li, *J. Therm. Anal. Calorim. 107 (***2012)** 471-475.
45.J. Tarábek, L. Kavan, L. Dunsch, M. Kalbac, *J. Phys. Chem. C 112 (***2008)** 13856-13861.

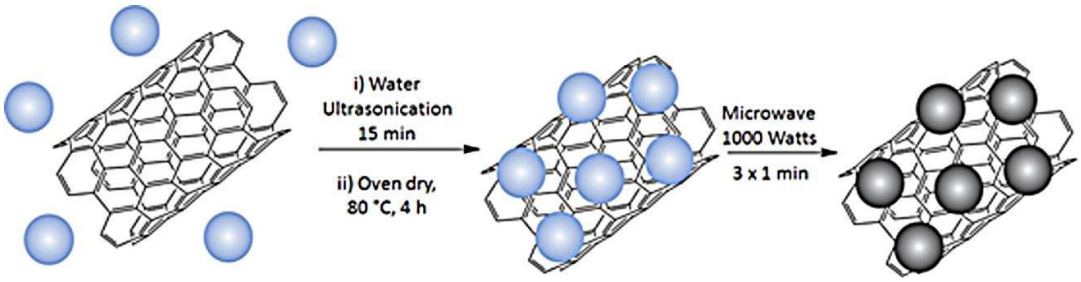

Fig. 1. A schematic representation showing the process of decoration of CNTs with tenorite nanoparticles. Blue spheres: CuAc; black spheres: CuO.

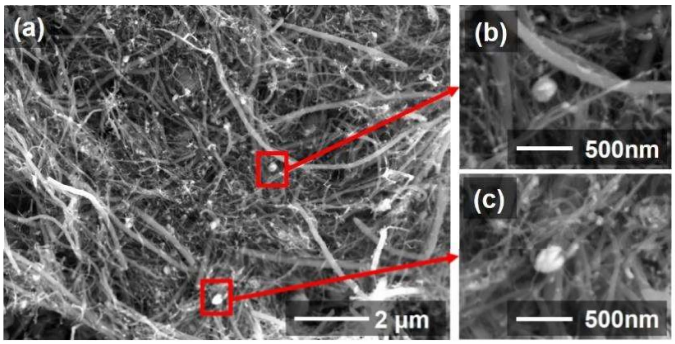

Fig. 2. SEM images of (a) MWCNTs decorated with CuO after three microwave treatments (CuAc loading 47.4 wt%) at low magnification, and (b and c) enlarged sections of image (a) showing individual nanoparticles of CuO.

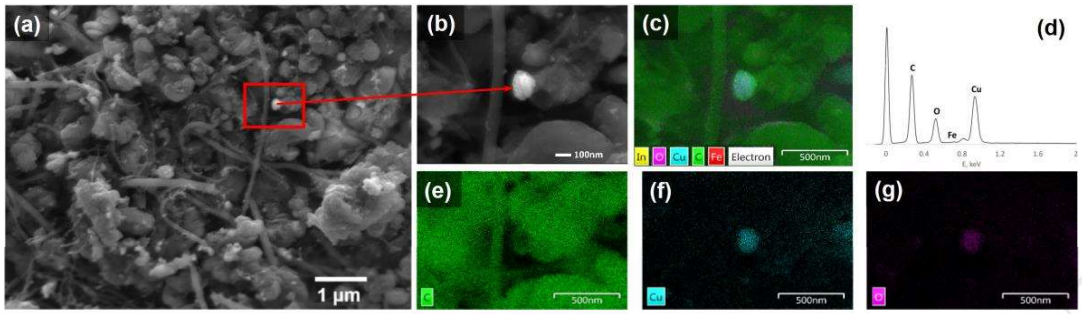

Fig. 3. SEM images of (a) MWCNTs decorated with CuO after three microwave treatments (47.4 wt% CuAc initial loading) at low magnification, (b) enlarged section of image (a) with a tenorite nanoparticle. (c) EDX map superimposed on SEM image (b) showing the distribution of carbon, copper, oxygen, iron and indium, (d) EDX spectrum for the framed area in image (b), and (e-g) EDX individual maps for the carbon, copper, and oxygen, respectively.

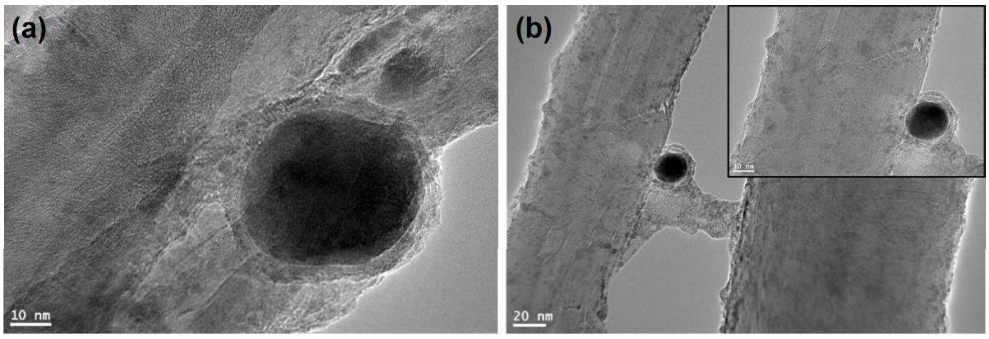

Fig. 4. TEM images of tenorite nanoparticles decorating MWCNTs from (a) 9.1 wt% and (b) 47.4 wt% CuAc initial loading.

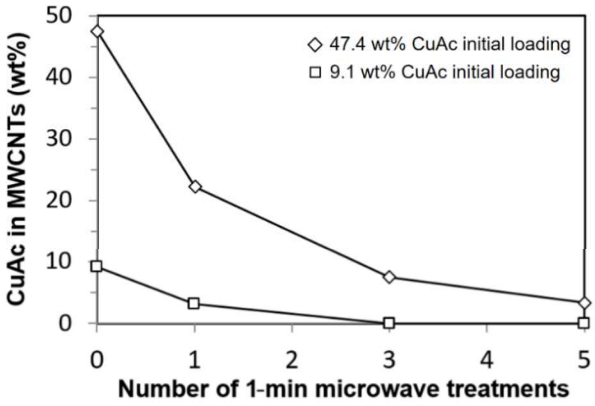

Fig. 5. Amount of copper acetate remaining uncovered in MWCNTs after an increasing number of 1-min microwave treatments. Comparison between two different initial loadings of CuAc: diamonds 47.4 wt%, squares 9.1 wt%.

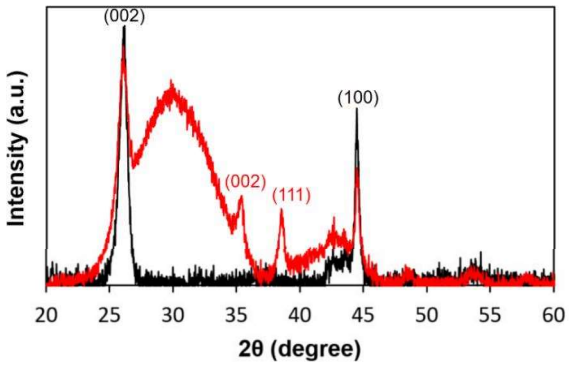

Fig. 6. XRD patterns of MWCNTs with 47.4 wt% (red) and without (black) added copper acetate, after three microwave treatments. Miller indices refer to CuO (red) and MWCNTs (black) reflections.

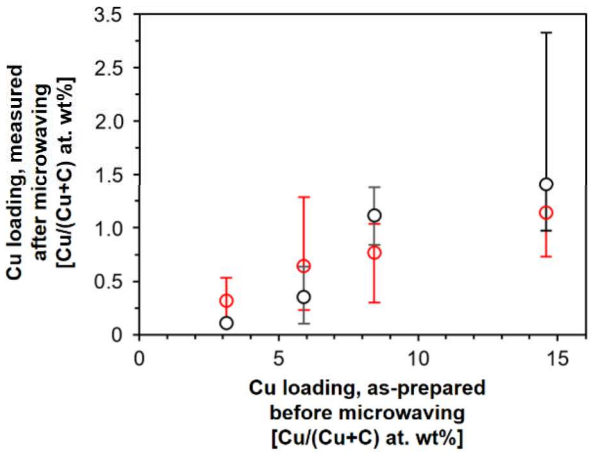

Fig. 7. Copper loading in MWCNT samples measured using EDX plotted against the amount of copper from CuAc used during preparation (Table 1). Black circles and bars correspond to before microwave treatment, whilst red circles and bars are after three microwave treatments. The range bars represent the upper and lower limits of the spread of data. Each analysis is expressed as the average of three probed areas.

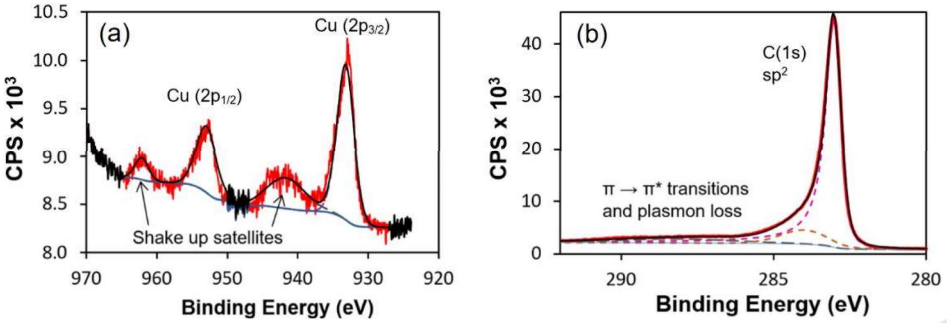

Fig. 8. (a) Representative Cu(2p) peaks from 90 wt% added CuAc sample after three microwave treatments, with fittings. (b) Representative C(1s) peak from 30 wt% added CuAc sample after three microwave treatments with fitting.

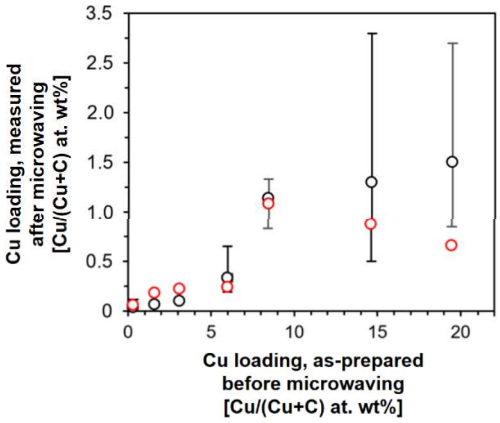

Fig. 9. Copper loading in MWCNT samples measured using EDX (black circles) and XPS (red circles) after three microwave treatments plotted against the amount of copper from CuAc used during preparation (Table 1). For EDX, the range bars represent the upper and lower limits of the spread of data from at least three measurements. For XPS, one region scan was taken for each sample.

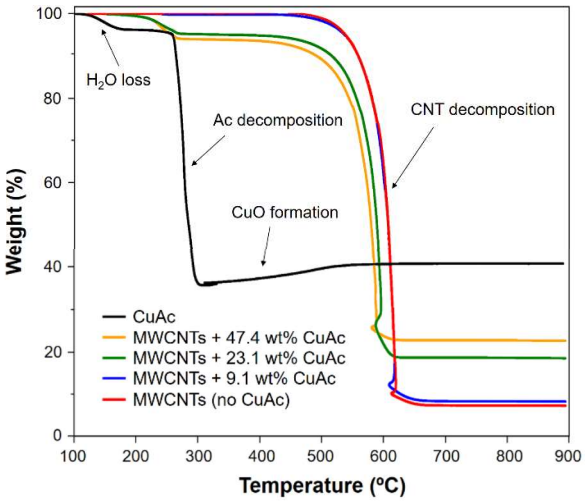

Fig. 10. TGA of pure copper acetate (black line), tenorite-decorated MWCNT samples after three microwave treatments (orange, green, and blue lines), and as received MWCNTs (red line).

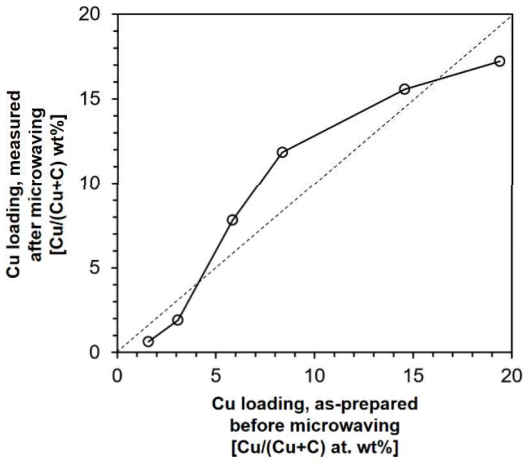

Fig. 11. Copper loading in MWCNT samples measured using TGA after three microwave treatments plotted against the amount of copper from CuAc used during preparation (Table 1). The dashed diagonal line represents the expected copper loading when the only process occurring while microwaving is the conversion of CuAc to tenorite, without loss of carbon.

Table 1. As-prepared loadings of copper acetate and copper in MWCNT samples. The amount of MWCNTs was fixed to 10 mg for all samples. Detailed calculations of Cu loadings are provided in Section 1 of the Supplementary Material (SM).

CuAc stock solution [mL]	CuAc loading [wt%]	Cu loading [Cu/(Cu+C) at. wt%]
9.0 (9.0 mg CuAc)	47.4	19.4
6.0 (6.0 mg CuAc)	37.5	14.6
3.0 (3.0 mg CuAc)	23.1	8.4
2.0 (2.0 mg CuAc)	16.7	5.9
1.0 (1.0 mg CuAc)	9.1	3.1
0.5 (0.5 mg CuAc)	4.8	1.6
0.1 (0.1 mg CuAc)	1.0	0.3